UDC 666.112.6

Yu.S. Hordieiev, Y.R. Kalishenko, A.V. Zaichuk

EFFECT OF LANTHANUM OXIDE SUBSTITUTION FOR ALUMINA ON THE STRUCTURE, THERMOPHYSICAL PROPERTIES, AND CRYSTALLIZATION OF BARIUM ALUMINOBOROSILICATE GLASSES

Ukrainian State University of Science and Technologies, Dnipro, Ukraine

Barium aluminoborosilicate glasses are promising precursors for celsian-based glass-ceramics, but their crystallization pathways must be controlled to obtain stable low-expansion phases. This study examines $BaO–Al_2O_3–B_2O_3–SiO_2$ glasses in which Al_2O_3 was progressively replaced by 0–9 wt.% La_2O_3. All quenched compositions were transparent, colorless, and X-ray amorphous, while infrared spectra showed only modest changes in the local borate–silicate vibrational environment. La_2O_3-for-Al_2O_3 substitution increased density from 3.75 to 4.01 g/cm^3, raised the linear coefficient of thermal expansion from 8.71 to 9.47 ppm/^{0}C, increased the dilatometric softening point from 652 to 665^{0}C, and decreased electrical volume resistivity at 150^{0}C by about two orders of magnitude. Differential thermal analysis showed multistep crystallization, with the first exothermic peaks near 746–758^{0}C. Heat-treated La-free glass crystallized mainly through a hexagonal $BaAl_2Si_2O_8$-rich assemblage with monoclinic $BaAl_2Si_2O_8$ and BaB_2O_4, whereas 9 wt.% La_2O_3 favored $BaSiO_3$ and monoclinic $BaAl_2Si_2O_8$ without clear hexagonal $BaAl_2Si_2O_8$ reflections. The novel contribution is demonstrating La_2O_3-for-Al_2O_3 substitution as a compositional lever for jointly tuning glass properties and redirecting crystallization away from a hexacelsian-dominated route toward a $BaSiO_3$–monoclinic celsian assemblage in BaO-rich aluminoborosilicate glasses.

Keywords: borosilicate glass, celsian, lanthanum oxide, crystallization, glass-ceramics.

DOI: 10.32434/0321-4095-2026-167-4-126-136

Introduction

Barium aluminoborosilicate glasses are important precursors to celsian-based glass-ceramics, especially those containing monoclinic $BaAl_2Si_2O_8$, a phase valued for high refractoriness, low and stable thermal expansion, chemical durability, and favorable dielectric properties. This combination makes celsian-based ceramics attractive candidates for high-temperature radio-transparent materials, including radome components for aviation and rocket systems, where low and stable permittivity and dielectric loss must be maintained during aerodynamic heating, as well as for fiber-reinforced ceramic-matrix composites and low-temperature co-fired ceramic (LTCC) substrates and dielectrics [1–3]. $BaO–Al_2O_3–B_2O_3–SiO_2$ glasses are particularly relevant in this context because they combine barium aluminosilicate crystallization chemistry with the processing advantages introduced by boron oxide [3]. Within this system, B_2O_3 lowers melting temperature and viscosity, widens the glass-forming region, and improves melt homogeneity, allowing dense, visually defect-free glasses to be cast

and subsequently devitrified into the desired crystalline assemblage.

The central difficulty is that $BaAl_2Si_2O_8$ is polymorphic, and the technologically preferred phase is rarely the one that forms first. On heating, crystallization commonly begins with metastable hexagonal $BaAl_2Si_2O_8$, or hexacelsian, whereas the stable low-expansion monoclinic celsian phase develops only through subsequent transformation at higher temperature [4]. This hexacelsian-to-celsian conversion is notoriously sluggish and often remains incomplete even after prolonged treatment near 1400^{0}C, and hexacelsian itself is undesirable because it undergoes a reversible transformation with a large volume change that degrades mechanical and dielectric performance [4]. Biasing devitrification toward monoclinic celsian, or suppressing the hexacelsian-dominated pathway, is therefore a central processing objective in the design of celsian-based glass-ceramics.

Crystallization can be steered by nucleating agents, mineralizers, and deliberate compositional substitution, all of which alter the local glass structure, the distribution of charge-compensating cations, and the relative accessibility of competing crystalline phases. Lanthanum oxide is an appealing compositional lever because La^{3+} can modify silicate and borosilicate networks through strong La–O interactions and changes in oxygen speciation [5,6]. Depending on the base composition and substitution scheme, La_2O_3 additions have been reported to increase density, alter thermal expansion and softening behavior, and modify crystallization tendency [6]. Yet the consequences of substituting La_2O_3 directly for network-participating Al_2O_3 in BaO-rich, celsian-forming aluminoborosilicate glasses remain poorly defined. This substitution is especially significant because it simultaneously introduces a rare-earth oxide and reduces the Al_2O_3 available for $BaAl_2Si_2O_8$ formation, thereby changing both the glass network and the stoichiometric competition among celsian, barium silicate, and barium borate phases.

Despite this potential, the specific effect of La_2O_3-for-Al_2O_3 substitution on BaO-rich aluminoborosilicate glasses remains insufficiently understood, particularly with respect to the coupled evolution of amorphous structure, thermophysical properties, electrical insulation behavior, and celsian-forming crystallization. This gap is important because the desired processing outcome is not simply crystallization, but selective crystallization toward stable low-expansion phases while preserving useful glass-forming ability and controllable thermal response. The purpose of the present work is therefore to determine how progressive substitution of La_2O_3 for Al_2O_3 affects the amorphous structure, density, thermal expansion, dilatometric softening, electrical volume resistivity, and crystallization pathway of $BaO–Al_2O_3–B_2O_3–SiO_2$ glasses intended as precursors for celsian-based glass-ceramics.

Materials and methods

Glasses in the $BaO–Al_2O_3–B_2O_3–SiO_2–La_2O_3$ system, hereafter denoted as BaAlBSiLa glasses, were prepared by the melt-quenching method. The base composition was selected from the low-melting eutectic region of the $BaO–Al_2O_3–SiO_2$ system and modified with B_2O_3 to reduce the melting temperature while retaining suitability for the development of $BaAl_2Si_2O_8$-containing glass-ceramics. The BaO-rich aluminoborosilicate composition, close to $57.3BaO–13.2Al_2O_3–9.1B_2O_3–20.4SiO_2$, is promising because its components can participate in crystallization reactions leading to celsian-containing phase assemblages during subsequent ceramic processing [7].

The nominal batch composition was $57.27BaO–(13.18–w)Al_2O_3–9.09B_2O_3–20.46SiO_2–wLa_2O_3$, where w=0; 3; 6; and 9 wt.%, corresponding to stepwise replacement of Al_2O_3 by La_2O_3 on a weight-percent basis. Reagent-grade $BaCO_3$, Al_2O_3, H_3BO_3, SiO_2, and La_2O_3 were used as raw materials. Their purities and suppliers were as follows: $BaCO_3$ (99.8%, Reachim), Al_2O_3 (99.7%, Plasma), H_3BO_3 (99.6%, Reachim), SiO_2 (99.6%, Novohim), and La_2O_3 (99.9%, Sigma-Aldrich). The starting materials were weighed according to the target compositions and thoroughly mixed to ensure batch homogeneity. The batches were melted in corundum crucibles at 1380^{0}C for 60 min in a SiC rod-heated furnace. The melts were cast into preheated molds to obtain rectangular bars with dimensions of 5×5×50 mm^3 and discs with a diameter of 30 mm. The samples were annealed at 600^{0}C for 4 h and then cooled to room temperature at 40^{0}C/h.

The glasses were designated according to their La_2O_3 content as BASL0, BASL3, BASL6, and BASL9. The corresponding nominal compositions, in wt.%, were BASL0: $57.27BaO–13.18Al_2O_3–9.09B_2O_3–20.46SiO_2$; BASL3: $57.27BaO–10.18Al_2O_3–9.09B_2O_3–20.46SiO_2–3La_2O_3$; BASL6: $57.27BaO–7.18Al_2O_3–9.09B_2O_3–20.46SiO_2–6La_2O_3$; and BASL9: $57.27BaO–4.18Al_2O_3–9.09B_2O_3–20.46SiO_2–9La_2O_3$.

Thermal characterization was performed by simultaneous thermal analysis using an STA300 Nexta instrument (Hitachi) at a heating rate of 10^{0}C/min to determine the crystallization peak temperature, T_c, from the exothermic maxima in the DTA curves. Push-rod dilatometry (GT-1000) was conducted at 3^{0}C/min to determine the dilatometric softening point, T_d, and the linear coefficient of thermal expansion, CTE.

Structural characterization was performed by X-ray diffraction (XRD) on a DRON-3M diffractometer with Co-Kα radiation and by Fourier-transform infrared spectroscopy (FTIR) on a Shimadzu IRSpirit-XT spectrometer equipped with a QATR-S accessory. FTIR spectra were recorded in the range 1800–350 cm^{-1} with a spectral resolution of 2 cm^{-1}, using 24 scans per measurement. Phase identification was carried out by matching the XRD reflections with reference patterns from the Powder Diffraction File database.

Glass density was determined by Archimedes' principle using n-decane (ρ=0.732 g/cm^3) as the immersion liquid and a Radwag AS 220 R2 microbalance. At least three measurements were performed for each sample, and the values were reproducible within ±0.01 g/cm^3. Electrical volume resistivity was measured on flat-parallel polished plates in a two-electrode cell with graphite contacts. Measurements were conducted over the temperature range 100–300°C at a heating rate of 10°C/min using an E6-13A high-resistance meter (teraohmmeter).

Results and discussion

Figure 1 provides an initial assessment of the glass formation and visual quality of the BaAlBSiLa series after melt quenching. The XRD patterns of BASL0, BASL3, BASL6, and BASL9 are characterized by broad diffuse maxima rather than narrow, well-resolved reflections, a feature commonly associated with X-ray-amorphous materials, while sharp peaks would indicate crystalline contributions. The principal diffuse feature lies in the low- to mid-angle region, centered approximately at 30–35° 2θ, and remains broadly similar as La_2O_3 progressively replaces Al_2O_3. Within the resolution of these measurements, no distinct crystalline peaks are observed, suggesting that La_2O_3 additions up to 9 wt.% do not induce detectable crystallization under the applied melting, casting, and annealing conditions. The as-cast samples shown in Fig. 1, right, were transparent and colorless across the whole series, with no visible bubbles, striae, or surface devitrification, indicating that the chosen melting and annealing schedule was suitable across the entire La_2O_3 substitution range. Overall, Figure 1 indicates that the selected BaAlBSiLa compositions retain a glassy character across the investigated La_2O_3 range, providing a suitable basis for comparing their thermal, physical, and electrical properties.

Having established that all four compositions are X-ray amorphous and visually homogeneous, Figure 2 examines whether La_2O_3-for-Al_2O_3 substitution produces measurable changes in the short-range vibrational response of the BaAlBSiLa network. All spectra contain broad, overlapping bands between

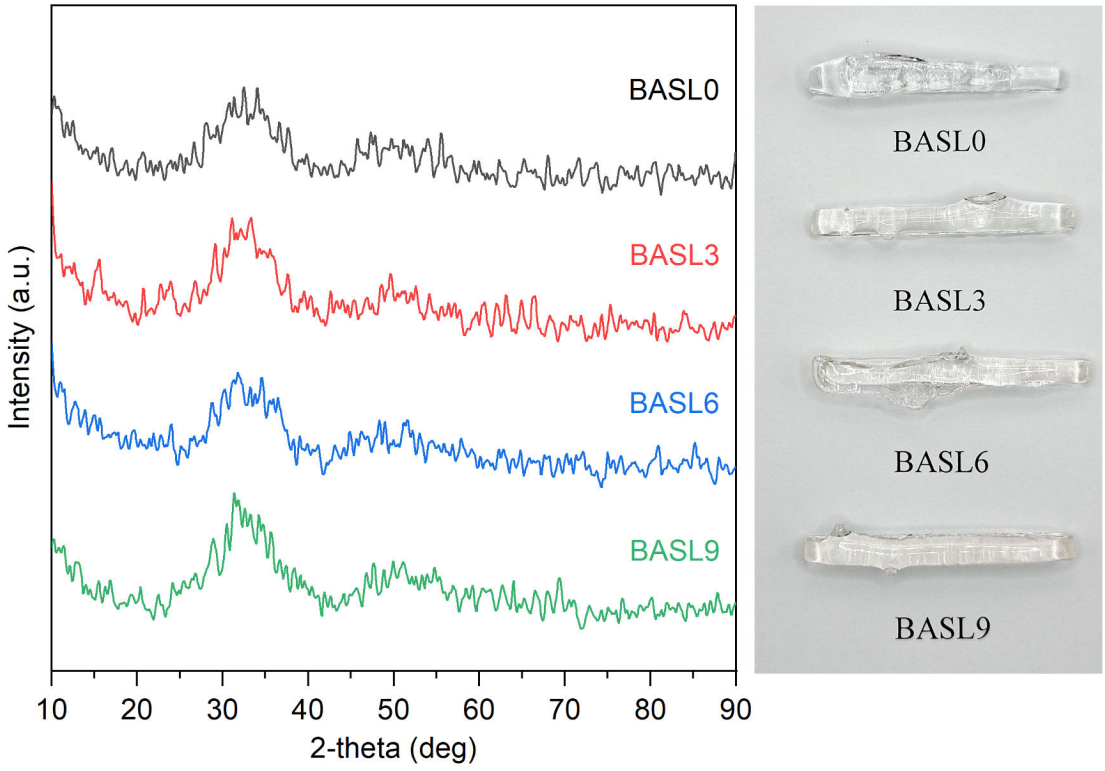

Fig. 1. X-ray pattenrs and photographs of melt-quenched BaAlBSiLa glasses with increasing La_2O_3 content

1600 and 400 cm^{-1}, consistent with the distribution of local vibrational environments expected for an amorphous mixed borate–silicate network, rather than the sharper and better-resolved bands typically associated with crystalline phases. Literature on borosilicate glasses commonly assigns bands in the 1150–1450 cm^{-1} region to B–O stretching vibrations of trigonal borate units, while the 900–1100 cm^{-1} region contains overlapping B–O and Si–O stretching contributions [8]. Bands near 700 cm^{-1} are generally associated with B–O–B bending vibrations in borate groups. The low-wavenumber component near 400–500 cm^{-1} may be attributed mainly to bending-type vibrations of the silicate network [9], such as Si–O–Si or O–Si–O motions associated with SiO_4 tetrahedra, although overlapping contributions from other network units cannot be excluded. On this basis, the small peak displacements observed here are best interpreted as evidence of a gradual change in the local borate–silicate vibrational environment as La_2O_3 replaces Al_2O_3, rather than as evidence for a major reorganization of the glass network. The persistence of broad, overlapping bands across the series suggests that La_2O_3 addition does not produce abrupt changes in the main FTIR features of the BaAlBSiLa glasses. Together, the XRD and FTIR results indicate that La_2O_3 addition does not produce detectable crystallization, but instead leads to modest changes in the local vibrational environment of the amorphous BaAlBSiLa network.

Despite the limited structural changes detected by XRD and FTIR, the physical and electrical properties respond predictably to La_2O_3-for-Al_2O_3 substitution, as shown in Fig. 3. The density increases steadily from 3.75 g/cm^3 for BASL0 to 4.01 g/cm^3 for BASL9 as La_2O_3 replaces Al_2O_3. This trend is expected primarily from the much higher molar mass of La_2O_3 relative to Al_2O_3, and is consistent with reported borosilicate systems in which density rises with increasing La_2O_3 content and decreases with increasing Al_2O_3 content [10]. In contrast, the logarithm of the electrical volume resistivity at 150°C decreased from $\log_{10}[\rho/(\Omega\cdot cm)]$=13.92 for BASL0 to 11.88 for BASL9, corresponding to a reduction by about two orders of magnitude. Even after this decrease, the resistivity values remained in the 10^{11}–10^{13} Ω·cm range, which is typical of highly insulating borosilicate-based glasses measured at comparable temperatures [11]. The decrease in resistivity suggests that La_2O_3-for-Al_2O_3 substitution lowers the resistance to thermally activated charge transport in the BaAlBSiLa glass matrix. This change may be related to a redistribution of charge-compensating cations and to modification of the amorphous network as Al_2O_3, which can form charge-balanced AlO_4 units, is progressively replaced by La_2O_3. The dilatometric data

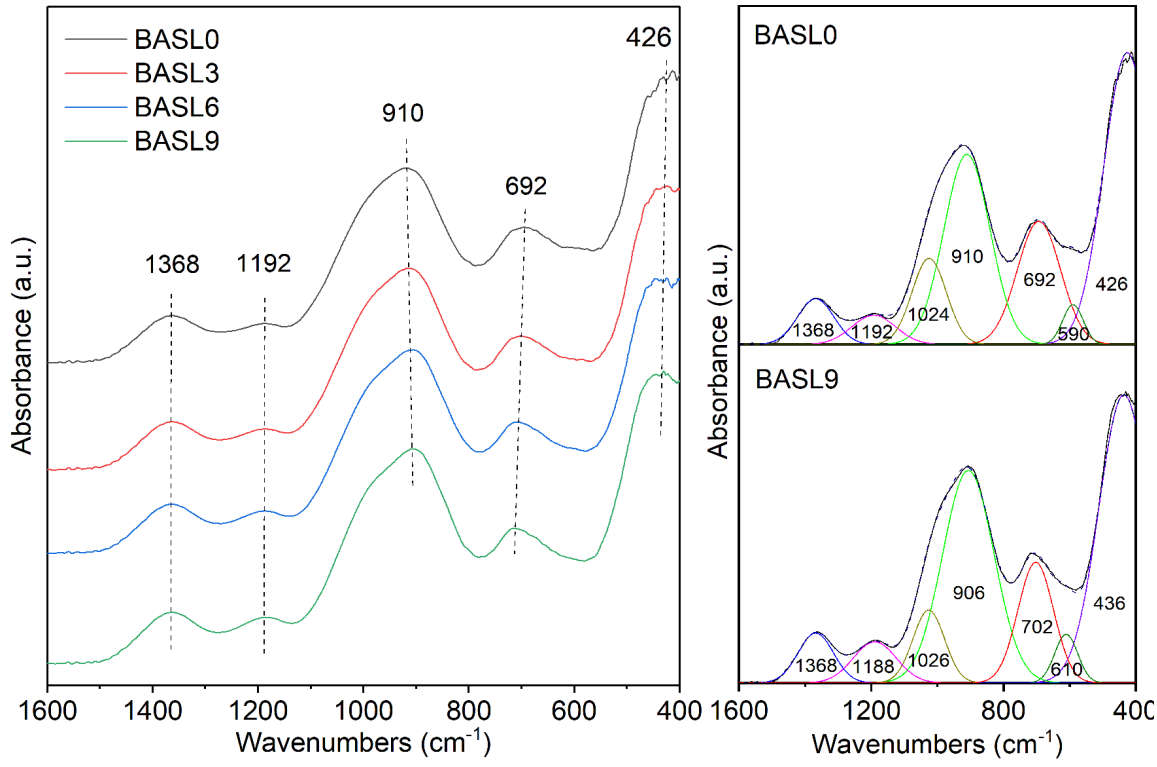

Fig. 2. Effect of La_2O_3-for-Al_2O_3 substitution on the FTIR response of BaAlBSiLa glasses

show that both the linear CTE and the softening point T_d rise with La_2O_3 content: CTE increases from 8.71 to 9.47 ppm/^{0}C, while T_d shifts from 652 to 665^{0}C. The increase in CTE indicates that La_2O_3-for-Al_2O_3 substitution increases the thermal expansivity of the glass below the softening range. One possible explanation is that Al_2O_3, which can participate in the glass network, is progressively replaced by La_2O_3, whose role in borosilicate glasses is often modifier-like. La_2O_3 additions have been reported [12] to alter borosilicate glass connectivity and thermal behavior, with the direction and magnitude of the effect depending strongly on the base composition and substitution scheme. The simultaneous rise in T_d may at first seem inconsistent with a simple network-depolymerization interpretation, since reduced network connectivity would generally be expected to lower the softening temperature. In the present glasses, however, the higher T_d may reflect the high charge and field strength of La^{3+}, which can produce relatively strong local La–O interactions with surrounding oxygens. These local cation–oxygen constraints may hinder cooperative structural rearrangement during softening and therefore retard viscous flow, shifting T_d to higher temperature even while the sub-T_d thermal expansion increases. Thus, the two trends appear to reflect different aspects of the glass response: the average thermoelastic behavior controls expansion below the softening range, whereas La-associated local constraints may influence the onset of viscous deformation. Overall, Figure 3 shows that La_2O_3 addition densifies the BaAlBSiLa glasses, lowers their electrical volume resistivity, and produces a modest upward shift in both CTE and T_d. These property changes provide the basis for interpreting the subsequent DTA results, particularly the thermal events associated with crystallization.

The DTA and post-heat-treatment XRD results show that La_2O_3 substitution affects both crystallization temperatures and the crystalline phases formed during heating. In Fig. 4, all compositions show a weak DTA endothermic/inflection feature at approximately 697–712^{0}C, which is tentatively assigned to the glass-transition or structural-relaxation region, followed by one or more exothermic events assigned to crystallization. The first exothermic peak remains in a narrow range of 746–758^{0}C, occurring at 756^{0}C for BASL0 and at about 758, 746, and 750^{0}C for BASL3,

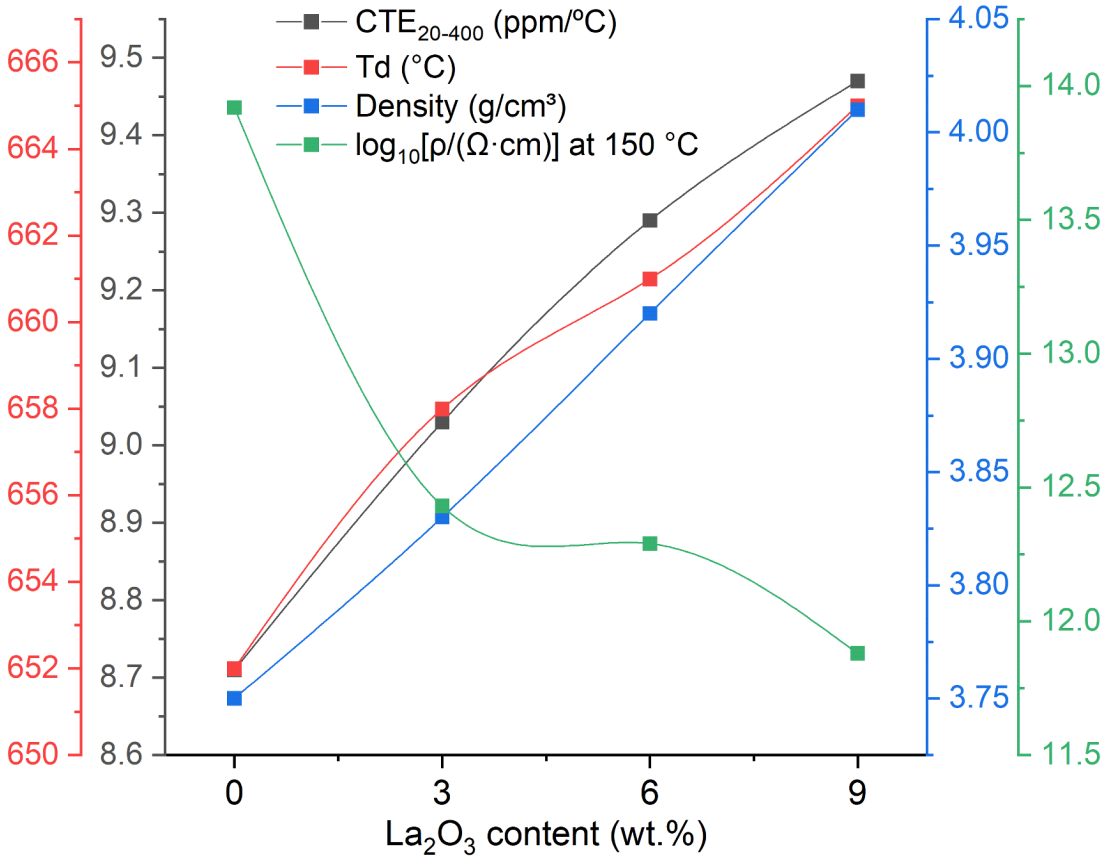

Fig. 3. Properties of BaAlBSiLa glasses as a function of La_2O_3 content

BASL6, and BASL9, respectively. Relative to BASL0, the peak is nearly unchanged for BASL3 and shifts slightly lower for BASL6 and BASL9. The higher-temperature events were more composition-dependent: BASL0 showed an additional effect at 810°C, BASL3 at 830°C, BASL6 at 1080°C, and BASL9 at 853 and 1054°C. This separation of thermal events suggests a multistep crystallization process rather than the formation of a single phase in one interval. Such behavior is consistent with barium aluminosilicate glass-ceramics, where DTA peaks near 800–820°C have been associated with celsian formation, and where the relative BaO/Al_2O_3 content influences crystallization temperature and phase development [13].

To identify which crystalline products correspond to the main DTA exotherms, BASL0 and BASL9 were heat-treated at temperatures corresponding to selected DTA peak temperatures, and the resulting XRD patterns are presented in Fig. 5. For BASL0 (Fig. 5a), both the 756°C and 810°C treatments produce well-resolved crystalline patterns containing prominent reflections assigned to hexagonal $BaAl_2Si_2O_8$ (Ref. code 01-077-0185), together with weaker reflections attributable to monoclinic $BaAl_2Si_2O_8$ (Ref. code 00-019-0090) and BaB_2O_4 (Ref. code 01-085-0914). The presence of both $BaAl_2Si_2O_8$ polymorphs, with hexacelsian giving the most prominent assigned reflections, agrees with earlier reports on barium aluminosilicate glasses, in which devitrification commonly yields hexacelsian first, while conversion to monoclinic celsian is promoted by suitable additives, mineralizers, nucleating agents, seed crystals, or extended thermal treatment. This behavior is generally attributed to the sluggish kinetics of the hexagonal-to-monoclinic transformation, which requires substantial structural rearrangement. From a processing perspective, direct formation of monoclinic celsian is preferable, since it avoids reliance on this sluggish transformation and favors the stable, low-expansion barium aluminosilicate phase sought in many glass-ceramic applications.

By contrast, BASL9 does not reproduce the BASL0 phase assemblage. After treatment at 750, 853, and 1054°C, the indexed reflections are attributed mainly to $BaSiO_3$ (Ref. code 00-021-0083) and

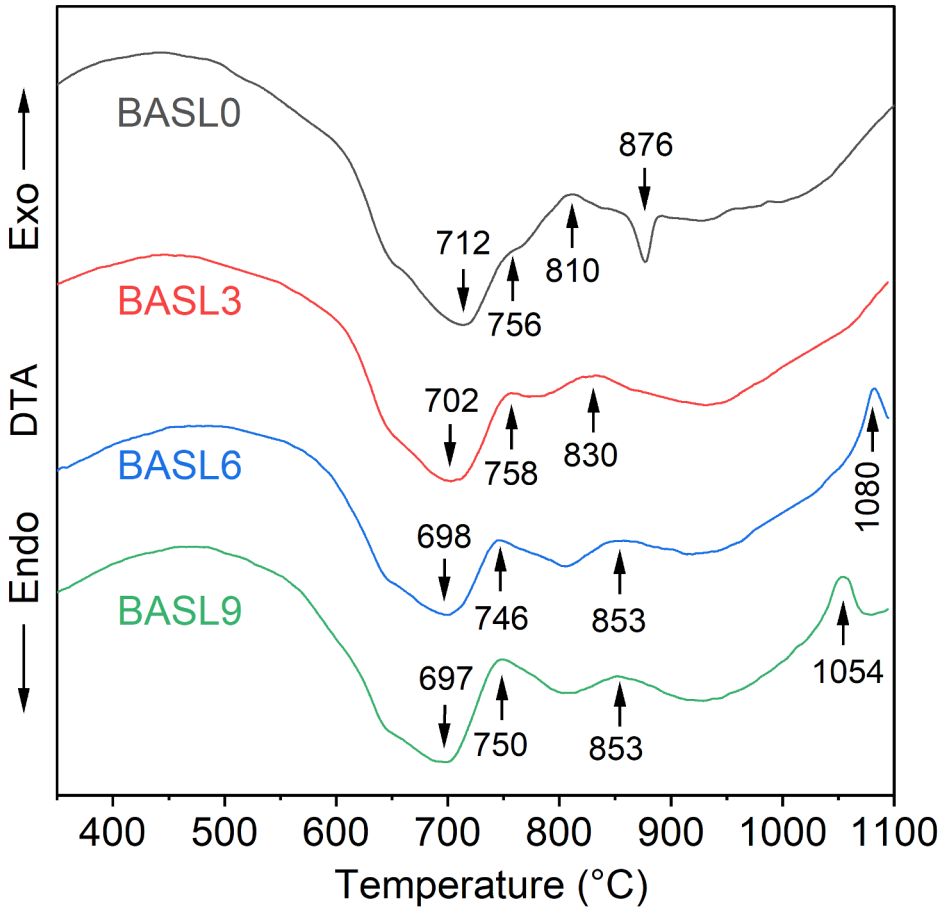

Fig. 4. Effect of La_2O_3-for-Al_2O_3 substitution on the DTA behavior of BaAlBSiLa glasses

monoclinic $BaAl_2Si_2O_8$, while strong, unambiguous reflections of hexagonal $BaAl_2Si_2O_8$ are not evident within the detection limits of the present XRD patterns (Fig. 5b). This result indicates that high La_2O_3 substitution changes the crystallization pathway rather than simply shifting the crystallization temperature. The appearance of $BaSiO_3$ is consistent with the high-La_2O_3, low-Al_2O_3 composition of BASL9: as Al_2O_3 is progressively replaced by La_2O_3, less alumina is available to combine with BaO and SiO_2 in stoichiometric $BaAl_2Si_2O_8$, so part of the Ba–Si component may crystallize separately as $BaSiO_3$. La_2O_3-for-Al_2O_3 substitution changes the competitive phase selection, but the reduced Al_2O_3 content also limits the stoichiometric capacity for $BaAl_2Si_2O_8$ formation. From a processing standpoint, the BASL9 result is significant because monoclinic celsian is generally the desired $BaAl_2Si_2O_8$ polymorph for low-expansion and thermally stable ceramic applications, whereas hexacelsian is less desirable because it can undergo polymorphic changes and because its conversion to monoclinic celsian is kinetically sluggish. The BASL9 patterns therefore suggest that La_2O_3-for-Al_2O_3 substitution changes the competitive crystallization reactions, suppressing the hexacelsian-dominated route observed in BASL0 and yielding a $BaSiO_3$–monoclinic celsian assemblage under the present heat-treatment conditions.

Following the phase identification by XRD, the FTIR spectra in Fig. 6 provide supporting vibrational evidence consistent with different crystallization paths for BASL0 and BASL9. In BASL0, treatment at 756 and 810°C converts the broad glass bands into more resolved features, consistent with increased structural ordering and with the crystalline products identified by XRD in Fig. 5a, where the strongest assigned reflections are associated with hexagonal $BaAl_2Si_2O_8$, accompanied by monoclinic $BaAl_2Si_2O_8$ and BaB_2O_4. The persistence of the high-wavenumber borate-related bands is consistent with the BaB_2O_4 contribution detected by XRD, since borate glasses and borate units commonly show B–O stretching contributions in the 1200–1500 cm^{-1} region and bending-related features near 700 cm^{-1}. At the same time, the bands between about 900 and 400 cm^{-1} are compatible with aluminosilicate and silicate vibrations expected for $BaAl_2Si_2O_8$-containing products. Literature on celsian-forming systems places Si–O stretching near 1035 cm^{-1}, Si–O–Al-related contributions in the 800–600 cm^{-1} region, and Si–O bending near 460 cm^{-1} [14]. The BASL9 spectra show a different evolution. After heat treatment at 750, 853, and especially 1054°C, the most evident bands occur mainly in the 809–962 cm^{-1} and 386–774 cm^{-1} regions, while the high-wavenumber borate-related bands appear less prominent than in BASL0. This redistribution is consistent with the XRD result in Fig. 5b, where BASL9 yielded mainly BaSiO and monoclinic $BaAl_2Si_2O_8$ rather than the hexacelsian-dominated path observed for BASL0. Reported barium silicate spectra [15] include features in the 600–700 cm^{-1} range, maxima near 731 and

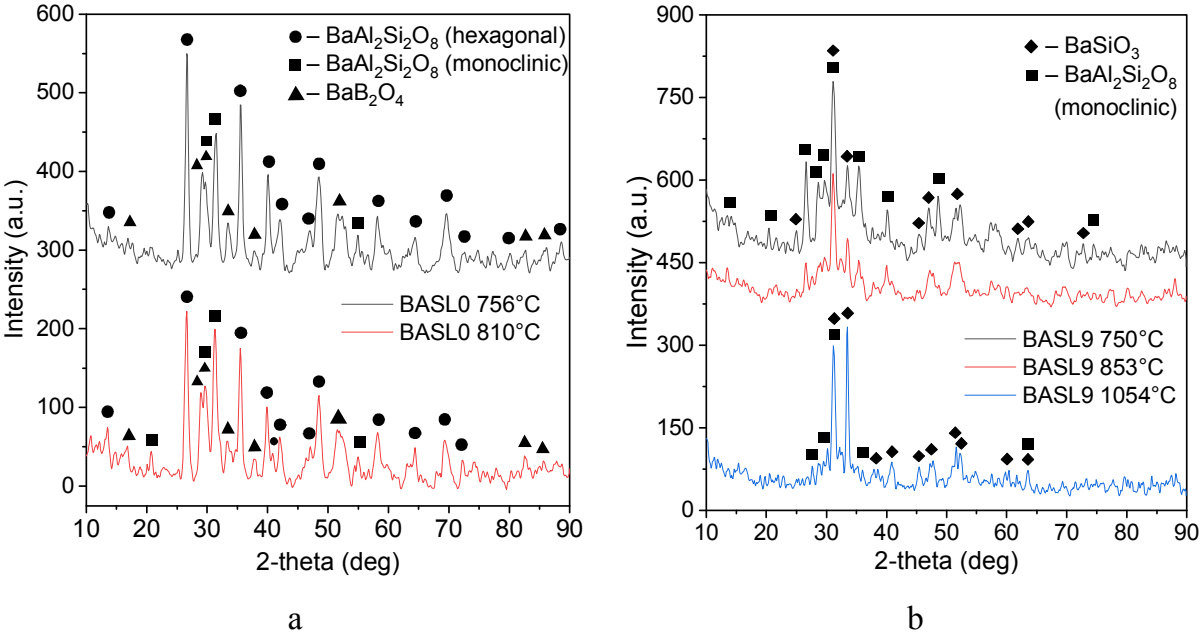

Fig. 5. XRD phase evolution of BASL0 (a) and BASL9 (b) after heat treatment

690 cm^{-1}, and deformation modes around 500 cm^{-1}, which helps rationalize the stronger low-wavenumber structure in BASL9. Thus, Figure 6 supports the main conclusion drawn from Fig. 5: La_2O_3 substitution does not merely shift crystallization temperatures, but changes the competitive phase development during heat treatment. These combined XRD and FTIR results provide the structural basis for the final conclusions on how La_2O_3 controls the processing response of BaAlBSiLa glass-ceramics.

Conclusions

La_2O_3-for-Al_2O_3 substitution preserved glass formation in the investigated BaO-rich aluminoborosilicate compositions while compositionally tuning their physical properties and crystallization products. All compositions containing 0; 3; 6; and 9 wt.% La_2O_3 remained visually homogeneous and X-ray amorphous after melt quenching and annealing, indicating that La_2O_3 contents up to 9 wt.% are compatible with stable glass preparation under the selected processing conditions.

The main property changes were consistent but moderate: density rose from 3.75 to 4.01 g/cm^3, thermal expansion increased from 8.71 to 9.47 ppm/^{0}C, and the dilatometric softening point shifted upward from 652 to 665^{0}C. Electrical volume resistivity at 150^{0}C decreased by about two orders of magnitude across the substitution series, although all compositions retained highly insulating behavior. These coupled trends are consistent with the replacement of network-forming Al_2O_3 by the heavier and more modifier-like La_2O_3 component, which increases glass density, changes charge-compensation environments, and modifies the thermal response of the amorphous network.

The most significant effect of La_2O_3 was the change in crystallization pathway. The La-free glass crystallized predominantly as hexagonal $BaAl_2Si_2O_8$, with weaker X-ray diffraction reflections attributable to monoclinic $BaAl_2Si_2O_8$ and BaB_2O_4. In contrast, the glass containing 9 wt.% La_2O_3 yielded mainly $BaSiO_3$ and monoclinic $BaAl_2Si_2O_8$ after heat treatment, with no strong evidence for dominant hexacelsian formation. La_2O_3 substitution therefore acts not only as a property modifier but also as a phase-selection tool, steering crystallization away from the hexacelsian-dominated route observed in the La-free glass toward a $BaSiO_3$—monoclinic celsian assemblage under the present heat-treatment conditions.

Conflict of interest

A.V. Zaichuk is an Editorial Board Member of the journal but was not involved in the peer-review process or the decision-making regarding this manuscript. All other authors declare no conflict of interest.

Acknowledgments

This work was supported by the Ministry of Education and Science of Ukraine (project No. 0126U000734).

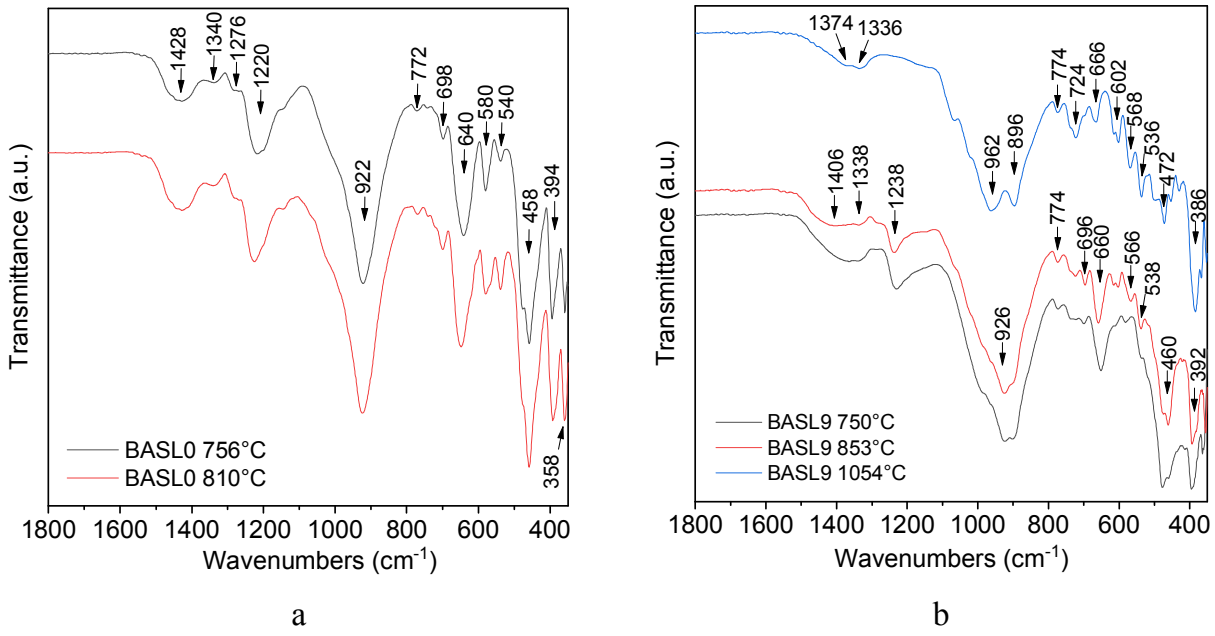

Fig. 6. FTIR spectra of BASL0 (a) and BASL9 (b) after heat treatment at selected crystallization temperatures

REFERENCES

1. *Ultra-high* frequency radio-transparent ceramics of celsian composition based on $BaO-Al_2O_3-B_2O_3-SiO_2$ glass: microstructure, physical and technical properties / Zaichuk A., Amelina A., Kalishenko Yu., Hordieiev Yu., Rudnieva L. // J. Chem. Technol. Metall. – 2022. – Vol.57. – No. 6. – P.1183-1194.

2. *Bansal N.P.* Celsian formation in fiber-reinforced barium aluminosilicate glass–ceramic matrix composites // Mater. Sci. Eng. A Struct. Mater. – 2003. – Vol.342. – No. 1-2. – P.23-27.

3. *Composite* material based on oxyfluoride barium boron-aluminosilicate glass and Al_2O_3 for LTCC technology / Kostanyan A.K., Manukyan H.G., Sargsyan K.A., Karakhanyan G.S., Alexanyan H.A., Knyazyan N.B. // Glass. Ceram. – 2025. – Vol.82. – No. 1-2. – P.88-92.

4. *Hyatt M.J., Bansal N.P.* Crystal growth kinetics in $BaOAl_2O_32SiO_2$ and $SrOAl_2O_32SiO_2$ glasses // J. Mater. Sci. – 1996. – Vol.31. – No. 1. – P.172-184.

5. *The structural* role of lanthanum oxide in silicate glasses / Gaddam A., Fernandes H.R., Tulyaganov D.U., Ferreira J.M.F. // J. Non Cryst. Solids. – 2019. – Vol.505. – P.18-27.

6. *Effects* of lanthanum oxide on the properties of barium-free alkaline-earth borosilicate sealant glass / Sasmal N., Garai M., Molla A.R., Tarafder A., Singh S.P., Karmakar B. // J. Non Cryst. Solids. – 2014. – Vol.387. – P.62-70.

7. *Radio-transparent* celsian ceramics modified with glass in a pseudoternary system $BaO-Al_2O_3-SiO_2$: synthesis, microstructure, thermal and physical properties / Zaichuk O.V., Amelina A.A., Kalishenko Y.R., Hordieiev Y.S. // Voprosy khimii i khimicheskoi tekhnologii. – 2024. – No. 5. – P.71-78.

8. *Effect* of replacement of CaO by La_2O_3 on the structure, thermal and dielectric properties of alkali-free aluminoborosilicate glasses / Wu W., Tian X., Zhang L., Liu X., Wu C., Gu G., Qu Y., Liang X., Yue Y., Kang J. // Ceramics–Silikaty. – 2023. – Vol.67. – No. 1. – P.73-80.

9. *Vibrational* spectroscopy analysis of silica and silicate glass networks / Liu H., Kaya H., Lin Y-T., Ogrinc A., Kim S.H. // J. Am. Ceram. Soc. – 2022. – Vol.105. – No. 4. – P.2355-2384.

10. *Karasik E.V., Hordieiev Y.S.,* Calculation of thermal expansion, glass transition temperature and glass density in the system $RO-Al_2O_3-B_2O_3-SiO_2$ (where RO=BaO, SrO, CaO, MgO, ZnO). // Voprosy Khimii i Khimicheskoi Tekhnologii. – 2020. – No. 6. – P.69-74.

11. *Structural*, electrical and thermal properties of borosilicate glass–alumina composites / Lima M.M.R.A., Monteiro R.C.C., Graзa M.P.F., Ferreira da Silva M.G. // J. Alloys Compd. – 2012. – Vol.538. – P.66-72.

12. *Hordieiev Y., Zaichuk A.* Impact of La_2O_3 substitution on the structural, thermal, and radiation shielding properties of sodium–barium borosilicate glasses // Int. J. Ceram. Eng. Sci. – 2025. – Vol.7. – Art. No. e70029.

13. *Thermodynamic* analysis of reactions of the celsian phase formation during the synthesis of thermal shock resistance ceramics based on eutectic glasses of the $BaO-Al_2O_3-SiO_2$ system / Zaichuk O., Amelina A., Hordieiev Y., Kalishenko Y., Ovchynnykov O., Basov Y., Sanin A., Kulyk O. // Voprosy Khimii i Khimicheskoi Tekhnologii. – 2023. – No. 3. – P.63-71.

14. *FTIR* study of the thermal transformation of barium-exchanged zeolite A to celsian / Aronne A., Esposito S., Ferone C., Pansini M., Pernice P. // J. Mater. Chem. – 2002. – Vol.12. – No. 10. – P.3039-3045.

15. *Properties* of barium silicate obtained by microwave–hydrothermal (M-H) method / Baghramyan V.V., Leonelli C., Mortalo C., Azatyan T.S., Petrosyan A.A., Ghazaryan A.A., Grigoryan T.V., Sargsyan A.A. // Appl. Sci. – 2026. – Vol.16. – No. 4. – Art. No. 2004.

Received 09.04.2026
Revised 23.06.2026
Accepted 13.07.2026
Published 10.08.2026

ВПЛИВ ЗАМІЩЕННЯ ОКСИДУ АЛЮМІНІЮ ОКСИДОМ ЛАНТАНУ НА СТРУКТУРУ, ТЕПЛОФІЗИЧНІ ВЛАСТИВОСТІ ТА КРИСТАЛІЗАЦІЮ БАРІЙАЛЮМОБОРОСИЛІКАТНИХ СТЕКОЛ

Ю.С. Гордєєв, Ю.Р. Калішенко, О.В. Зайчук

Барійалюмоборосилікатні стекла є перспективними прекурсорами для склокераміки на основі цельзіану, однак шляхи кристалізації цих стекол необхідно контролювати для отримання стабільних фаз із низьким коефіцієнтом теплового розширення. У роботі досліджено стекла системи $BaO-Al_2O_3-B_2O_3-SiO_2$, у яких Al_2O_3 поступово заміщували 0–9 мас.% La_2O_3. Усі загартовані склади були прозорими, безбарвними та рентгеноаморфними, тоді як інфрачервоні спектри засвідчили лише помірні зміни у локальному вібраційному оточенні боратно-силікатної сітки. Заміщення Al_2O_3 на La_2O_3 підвищувало густину з 3,75 до 4,01 г/см^3, збільшувало лінійний коефіцієнт теплового розширення з 8,71 до 9,47 ppm/^{0}C, підвищувало дилатометричну температуру розм'якшення з 652 до 665^{0}C і знижувало питомий об'ємний електричний опір при 150^{0}C приблизно на два порядки. Диференціальний термічний аналіз показав багатостадійну кристалізацію з першими екзотермічними піками в діапазоні 746–758^{0}C. Термооброблене скло без лантану кристалізувалося з формуванням фазового складу, у якому переважав гексагональний $BaAl_2Si_2O_8$, а також були наявні моноклінний $BaAl_2Si_2O_8$ і BaB_2O_4, тоді як уведення 9 мас.% La_2O_3 сприяло утворенню $BaSiO_3$ і моноклінного $BaAl_2Si_2O_8$ без чітких рефлексів гексагонального $BaAl_2Si_2O_8$. Новизна роботи полягає в обґрунтуванні заміщення Al_2O_3 на La_2O_3 як ефективного композиційного підходу до одночасного регулювання властивостей скла та спрямування кристалізації від переважного утворення гексацельзіану до формування фазового складу, представленого $BaSiO_3$ і моноклінним цельзіаном, в алюмоборосилікатних стеклах із високим вмістом BaO.

Ключові слова: боросилікатне скло, цельзіан, оксид лантану, кристалізація, склокераміка.

EFFECT OF LANTHANUM OXIDE SUBSTITUTION FOR ALUMINA ON THE STRUCTURE, THERMOPHYSICAL PROPERTIES, AND CRYSTALLIZATION OF BARIUM ALUMINOBOROSILICATE GLASSES

Yu.S. Hordieiev *, Y.R. Kalishenko, A.V. Zaichuk

Ukrainian State University of Science and Technologies, Dnipro, Ukraine

* **e-mail: yuriihordieiev@gmail.com**

Barium aluminoborosilicate glasses are promising precursors for celsian-based glass-ceramics, but their crystallization pathways must be controlled to obtain stable low-expansion phases. This study examines $BaO-Al_2O_3-B_2O_3-SiO_2$ glasses in which Al_2O_3 was progressively replaced by 0–9 wt.% La_2O_3. All quenched compositions were transparent, colorless, and X-ray amorphous, while infrared spectra showed only modest changes in the local borate–silicate vibrational environment. La_2O_3-for-Al_2O_3 substitution increased density from 3.75 to 4.01 g/cm^3, raised the linear coefficient of thermal expansion from 8.71 to 9.47 ppm/^{0}C, increased the dilatometric softening point from 652 to 665^{0}C, and decreased electrical volume resistivity at 150^{0}C by about two orders of magnitude. Differential thermal analysis showed multistep crystallization, with the first exothermic peaks near 746–758^{0}C. Heat-treated La-free glass crystallized mainly through a hexagonal $BaAl_2Si_2O_8$-rich assemblage with monoclinic $BaAl_2Si_2O_8$ and BaB_2O_4, whereas 9 wt.% La_2O_3 favored $BaSiO_3$ and monoclinic $BaAl_2Si_2O_8$ without clear hexagonal $BaAl_2Si_2O_8$ reflections. The novel contribution is demonstrating La_2O_3-for-Al_2O_3 substitution as a compositional lever for jointly tuning glass properties and redirecting crystallization away from a hexacelsian-dominated route toward a $BaSiO_3$–monoclinic celsian assemblage in BaO-rich aluminoborosilicate glasses.

Keywords: borosilicate glass; celsian; lanthanum oxide; crystallization; glass-ceramics.

REFERENCES

1. Zaichuk A, Amelina A, Kalishenko Yu, Hordieiev Yu, Rudnieva L. Ultra-high frequency radio-transparent ceramics of celsian composition based on $BaO-Al_2O_3-B_2O_3-SiO_2$ glass: microstructure, physical and technical properties. *J Chem Technol Metall.* 2022; 57(6): 1183-1194.

2. Bansal NP. Celsian formation in fiber-reinforced barium aluminosilicate glass–ceramic matrix composites. *Mater Sci Eng A Struct Mater.* 2003; 342(1-2): 23-27. doi: 10.1016/s0921-5093(02)00313-1.

3. Kostanyan AK, Manukyan HG, Sargsyan KA, Karakhanyan GS, Alexanyan HA, Knyazyan NB. Composite material based on oxyfluoride barium boron-aluminosilicate glass and Al_2O_3 for LTCC technology. *Glass Ceram.* 2025; 82(1-2): 88-92. doi: 10.1007/s10717-025-00753-x.

4. Hyatt MJ, Bansal NP. Crystal growth kinetics in $BaOAl_2O_32SiO_2$ and $SrOAl_2O_32SiO_2$ glasses. *J Mater Sci.* 1996; 31(1): 172-184. doi: 10.1007/bf00355142.

5. Gaddam A, Fernandes HR, Tulyaganov DU, Ferreira JMF. The structural role of lanthanum oxide in silicate glasses. *J Non Cryst Solids.* 2019; 505: 18-27. doi: 10.1016/j.jnoncrysol.2018.10.023.

6. Sasmal N, Garai M, Molla AR, Tarafder A, Singh SP, Karmakar B. Effects of lanthanum oxide on the properties of barium-free alkaline-earth borosilicate sealant glass. *J Non Cryst Solids*. 2014; 387: 62-70. doi: 10.1016/j.jnoncrysol.2013.12.030.

7. Zaichuk OV, Amelina AA, Kalishenko YR, Hordieiev YS. Radio-transparent celsian ceramics modified with glass in a pseudoternary system $BaO–Al_2O_3–SiO_2$: synthesis, microstructure, thermal and physical properties. *Voprosy Khimii i Khimicheskoi Tekhnologii*. 2024; (5): 71-78. doi: 10.32434/0321-4095-2024-156-5-71-78.

8. Wu W, Tian X, Zhang L, Liu X, Wu C, Gu G, et al. Effect of replacement of CaO by La_2O_3 on the structure, thermal and dielectric properties of alkali-free aluminoborosilicate glasses. *Ceramics–Silikaty*. 2023; 67(1): 73-80. doi: 10.13168/cs.2023.0004.

9. Liu H, Kaya H, Lin YT, Ogrinc A, Kim SH. Vibrational spectroscopy analysis of silica and silicate glass networks. *J Am Ceram Soc*. 2022; 105(4): 2355-2384. doi: 10.1111/jace.18206.

10. Karasik EV, Hordieiev YS, Calculation of thermal expansion, glass transition temperature and glass density in the system $RO–Al_2O_3–B_2O_3–SiO_2$ (where RO=BaO, SrO, CaO, MgO, ZnO). *Voprosy Khimii i Khimicheskoi Tekhnologii*. 2020; (6): 69-74. doi: 10.32434/0321-4095-2020-133-6-69-74.

11. Lima MMRA, Monteiro RCC, Graca MPF, Ferreira da Silva MG. Structural, electrical and thermal properties of borosilicate glass–alumina composites. *J Alloys Compd*. 2012; 538: 66-72. doi: 10.1016/j.jallcom.2012.05.024.

12. Hordieiev Y, Zaichuk A. Impact of La_2O_3 substitution on the structural, thermal, and radiation shielding properties of sodium–barium borosilicate glasses. *Int J Ceram Eng Sci*. 2025; 7: e70029. doi: 10.1002/ces2.70029.

13. Zaichuk O, Amelina A, Hordieiev Y, Kalishenko Y, Ovchynnykov O, Basov Y, et al. Thermodynamic analysis of reactions of the celsian phase formation during the synthesis of thermal shock resistance ceramics based on eutectic glasses of the $BaO–Al_2O_3–SiO_2$ system. *Voprosy Khimii i Khimicheskoi Tekhnologii*. 2023; (3): 63-71. doi: 10.32434/0321-4095-2023-148-3-63-71.

14. Aronne A, Esposito S, Ferone C, Pansini M, Pernice P. FTIR study of the thermal transformation of barium-exchanged zeolite A to celsian. *J Mater Chem*. 2002; 12(10): 3039-3045. doi: 10.1039/b203859e.

15. Baghramyan VV, Leonelli C, Mortalo C, Azatyan TS, Petrosyan AA, Ghazaryan AA, et al. Properties of barium silicate obtained by microwave–hydrothermal (M-H) method. *Appl Sci*. 2026; 16(4): 2004. doi: 10.3390/app16042004.